

# Marine predator migration during range expansion: Humboldt squid *Dosidicus gigas* in the northern California Current System

J. S. Stewart<sup>1,\*</sup>, E. L. Hazen<sup>2,3</sup>, D. G. Foley<sup>2,3</sup>, S. J. Bograd<sup>2</sup>, W. F. Gilly<sup>1</sup>

<sup>1</sup>Hopkins Marine Station of Stanford University, 120 Oceanview Boulevard, Pacific Grove, California 93950, USA

<sup>2</sup>Environmental Research Division, NMFS Southwest Fisheries Science Center, NOAA, 1352 Lighthouse Avenue, Pacific Grove, California 93950, USA

<sup>3</sup>Joint Institute for Marine and Atmospheric Research, University of Hawaii at Manoa, 1000 Pope Rd., Honolulu, Hawaii 96822, USA

**ABSTRACT:** Humboldt squid *Dosidicus gigas* have undergone a major range expansion in the northern California Current System (CCS) during the last decade. These squid are thought to migrate annually from Mexican waters into the CCS where they prey on many species, including several that support lucrative fisheries; however, swimming capabilities and features of long-distance horizontal migrations are not well understood. In the present study, adult Humboldt squid were tagged off central California with pop-up archival transmitting (PAT) tags ( $n = 5$ ). All squid exhibited diel vertical migrations and swam south or offshore (west) during tag deployment (2.7 to 17.6 d). One squid swam south at least  $34 \text{ km d}^{-1}$  for  $>17$  d and crossed into Mexican waters, which is the highest sustained velocity and the longest horizontal migration observed thus far for Humboldt squid. Results from a simple model to estimate the daily locations and velocities of each squid throughout the deployments suggest an average velocity of  $\sim 37 \text{ km d}^{-1}$  and a maximum of  $\sim 50 \text{ km d}^{-1}$ . Additionally, the model suggests that one squid made a bidirectional movement (first north and then returning south) that was not evident from deployment and pop-up positions alone. This study provides insight into Humboldt squid migratory capabilities that are relevant to seasonal migrations and episodic range expansions, both of which are crucial to future interactions of this species with ecosystems and fisheries.

**KEY WORDS:** California Current System · Jumbo squid · Range expansion · Satellite tagging · Swimming velocity

— Resale or republication not permitted without written consent of the publisher —

## INTRODUCTION

Long-term warming and natural climatic oscillations affect the ranges and migratory patterns of mobile organisms in both terrestrial and marine ecosystems (Chavez et al. 2003, Parmesan 2006). In marine environments, modified migratory behaviors can be associated with many factors including temperature (Perry et al. 2005), dissolved oxygen (Stramma et al. 2012), and timing of seasonal events such as phytoplankton blooms (Edwards & Richardson 2004)

and coastal upwelling (Bograd et al. 2009). Changes in the timing and routes of migrating predators can potentially lead to a myriad of effects on marine ecosystems and fisheries by altering the dynamic interactions with the predators and prey encountered during such migrations.

The California Current System (CCS) in the north-eastern Pacific Ocean is an upwelling-driven environment of high biodiversity and serves as a migratory pathway for many pelagic predators (Block et al. 2011) and forage fishes (e.g. Emmett et al. 2005,

\*Email: jules32@stanford.edu

Agostini et al. 2006), some of which are targeted by economically important fisheries. Recent large-scale changes in distribution and migration of pelagic species in the CCS have been attributed to delays in the onset of coastal upwelling (Brodeur et al. 2006) and shoaling of the oxygen minimum zone (Koslow et al. 2011), and long-term climate change is predicted to exacerbate these processes (Bograd et al. 2008, García-Reyes & Largier 2010, Deutsch et al. 2011, Iles et al. 2012). In addition, any effects of long-term climate change on migration routes in the CCS will also be impacted by natural oscillations such as Pacific Decadal Oscillation (PDO) and El Niño Southern Oscillation (ENSO), but interactions of these multiple drivers are not well understood (Yeh et al. 2009, Boucharel et al. 2011, Choi et al. 2011).

Humboldt (or jumbo) squid *Dosidicus gigas*, a large predator of significant commercial importance (FAO 2012), greatly expanded the northern extent of its range in the eastern Pacific Ocean from the previous northern extent in Mexico after the 1997/1998 ENSO event, first to Monterey Bay, CA (~35°N) (Gilly 2006, Zeidberg & Robison 2007) and then further north as far as southeastern Alaska (~60°N) (Cosgrove 2005, Brodeur et al. 2006, Wing 2006). Episodic range extensions of this sort may be characteristic of this species (Litz et al. 2011, Mazzillo et al. 2011), and success in exploiting new environments is undoubtedly aided by a short life cycle (1 to 2 yr), fast growth rate, high fecundity, flexible feeding strategy, and tolerance of environmental variability (Nigmatullin et al. 2001, Gilly & Markaida 2007, Jackson & O'Dor 2007).

During this recent range extension, Humboldt squid have been present in large numbers, and regional acoustic surveys (35–55°N) in 2009 indicated a biomass in excess of 10<sup>6</sup> t, a value comparable to that of Pacific hake *Merluccius productus* (Stewart & Hamel 2010), a commercially significant species in the same region with average annual landings of ~300 000 t from 2004 to 2009 (in FAO Area 67; FishStat 2012). *Dosidicus gigas* preys on hake in the northern CCS (Field et al. 2007, 2012), and this, as well as indirect interactions (Holmes et al. 2008), has potential economic consequences for the fishery, which is the largest on the US west coast (Stewart & Hamel 2010, FishStat 2012). The diet of Humboldt squid in the northern CCS also includes other species that constitute lucrative fisheries including California market squid *Doryteuthis* (formerly *Loligo*) *opalescens*, Pacific sardine *Sardinops sagax*, Pacific herring *Clupea pallasii*, several species of rockfish *Sebastodes* spp., and salmon *Oncorhynchus* spp. (Field et al. 2007, 2012, Braid et al. 2012). Humboldt squid are also prey to many top predators and have been identified as one of the 2 most important prey items in the diets of mako sharks *Isurus oxyrinchus* and blue sharks *Prionace glauca*, when this squid is abundant off California (Prete et al. 2012). Changes in the population size of *D. gigas*, thus, have the potential for exerting both top-down and bottom-up ecological consequences, although the magnitude of these impacts remains to be quantified.

The timing of encounters of *Dosidicus gigas* with the above prey and predators, along with size and maturity information throughout the CCS, has led to the hypothesis that Humboldt squid undergo an annual feeding migration into the northern CCS during summer and fall before returning south to Mexico to spawn in late fall or early winter (Field et al. 2012). Horizontal distances involved during this proposed migration would be at least 2750 km each way, conservatively assuming that squid migrate from the Pacific coast off Baja California where spawning occurs (27°N; Camarillo-Coop et al. 2007, Ramos-Castillejos et al. 2010) to Vancouver Island in British Columbia where adults are frequently encountered (49°N; Holmes et al. 2008, Braid et al. 2012). However, it is unknown how quickly Humboldt squid can cover such distances. The tendency for Humboldt squid to reside at a constant dim light-level (Gilly et al. 2012) renders light data from pop-up archival transmitting (PAT) tags on Humboldt squid essentially useless for geolocation (Gilly et al. 2006, Bazzino et al. 2010), and current estimates of horizontal movement by *D. gigas* are, therefore, based solely on deployment and end positions of PAT tags. This approach has suggested that Humboldt squid can swim at least 33 km d<sup>-1</sup> and that they can maintain this activity in a specific direction for at least 3 d (Gilly et al. 2006).

This study investigates the horizontal movements of Humboldt squid in the northern CCS to gain a better understanding of their long-distance migratory behavior and sustained swimming velocities. We deployed PAT tags on large, adult Humboldt squid in the autumn off central California to determine whether squid would swim south as would be expected under Field et al.'s (2012) putative migration scenario. We developed a simple modeling approach to estimate daily movement and velocities of tagged Humboldt squid based on tag and remote-sensing data. This is the first study directly investigating horizontal movements and swimming capabilities of Humboldt squid in their newly expanded range.

## MATERIALS AND METHODS

### Tagging

Nine adult Humboldt squid were tagged in the autumn off central California during this study: 3 in October 2008 off Cordell Bank and 6 in November 2009 near Monterey Bay. Squid were fished with weighted luminescent jigs (0.35 m in length) using rod and reel, carefully brought onboard by lifting the jig with a heavy monofilament leader, and immediately placed in a large cooler of seawater at ambient surface temperature where they were held in place by hand during the tagging procedure. Tags were attached in a manner similar to that described previously (Gilly et al. 2006), which also discussed the potentially deleterious effects of tagging. The present study attempted to improve the procedure by securing the tag to a small plastic platform rather than directly to the squid. This platform had 2 sharpened nylon screws (1/4-20) that were pushed through the fin from the ventral surface as close to the gladius as possible and secured with nylon nuts and washers on the dorsal surface. Thus, the platform remained on the squid after the tag detached at its programmed time. This procedure decreased the time required to attach the tag to the animal, and squid were released fins-first into the sea (to remove any air from the mantle cavity) from the vessel's swim step within 3 min of capture. Of the 9 tags deployed, 5 popped up and reported to Argos after archiving data (Fig. 1, Table 1).

All tags were Mk10 pop-up archival transmitting tags (PAT; Wildlife Computers) with 0.5 m and 0.05°C resolution in depth and

temperature, respectively. Tags were programmed to archive pressure (depth) and temperature at the highest resolution possible (1 Hz) and also to transmit data to the Système Argos following pop-up also at the highest resolution possible (0.0133 Hz) so that time-series data would be available even if the tag was not recovered. Programming the tags in this way allowed for fine-scale analysis of vertical velocities associated with jet propulsion (Gilly et al. 2006,

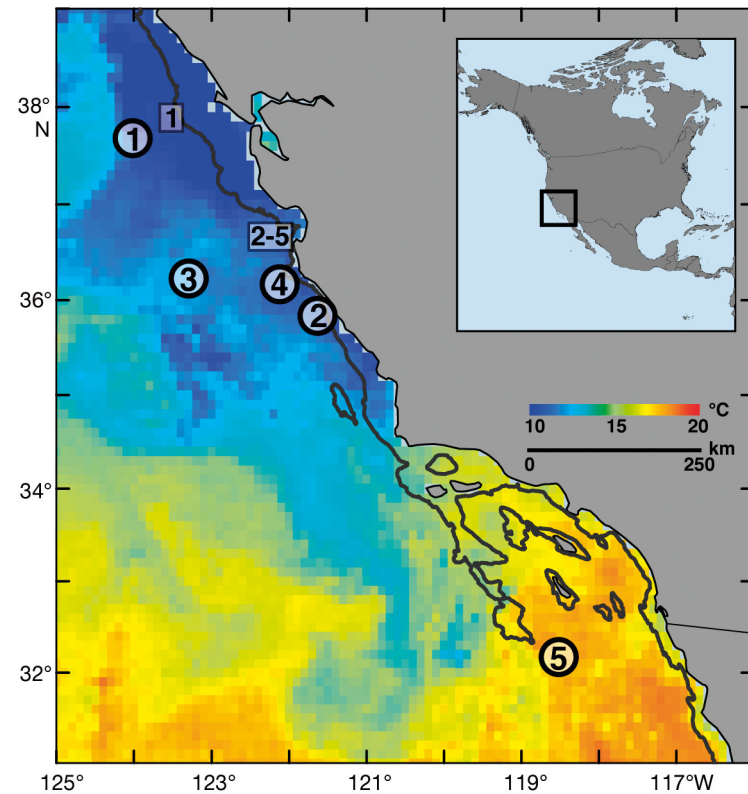


Fig. 1. Map of successful tagging in California. Numbers with boxes show deployment locations, and numbers with circles show corresponding pop-up locations for each tag (numbering as in Table 1). The black line identifies the 500 m contour line. CCS-1 was deployed in 2008, and CCS-2, 3, 4 and 5 were deployed in 2009. Remotely-sensed SST data is overlaid for November 5, 2009

Table 1. *Dosidicus gigas*. Deployment and pop-up information for 5 tagged Humboldt squid in California. CCS-1 was the only tag physically recovered. DML: dorsal mantle length.

Squid	TagID	DML (m)	Deployment			Pop-up			Sampling time (d)
			Date (mm/dd/yy)	Position °N	Position °W	Date (mm/dd/yy)	Position °N	Position °W	
CCS-1	83046_08	0.68	10/12/08	37.91	123.48	10/15/08	37.65	123.99	2.7
CCS-2	83046_09	0.74	09/30/09	36.71	122.03	10/14/09	35.85	121.50	12.7
CCS-3	83052_09	0.67	11/05/09	36.59	122.06	11/12/09	36.23	123.30	5.7
CCS-4	64004_09	0.69	11/05/09	36.58	122.05	11/10/09	36.18	122.09	3.0
CCS-5	83051_09	0.79	11/05/09	36.58	122.06	11/24/09	32.09	118.45	17.6

2012), but reduced the maximum possible length of tag deployment to 17 d. This trade-off was deemed acceptable because our previous experience demonstrated that tags deployed for times longer than 30 d inevitably detached prematurely (Gilly et al. 2006, 2012, Bazzino et al. 2010). Premature detachment leads to uncertainty in the end-point (pop-up) location, because the detached tag floats to the surface and drifts for an obligatory period of least 24 h before transmission to Argos can be enabled.

### Movement analyses

#### Direct distances

Net or direct horizontal distances traveled were calculated using the distance between the tag deployment and pop-up locations as described later in 'Environmental data'. Distance, along with the total days of deployment, gave an average daily velocity that reflected a minimum daily rate that would allow the squid to travel between these 2 points. These results are reported and discussed as 'direct' values.

#### Modeling daily locations

Daily horizontal movement was further investigated using a heuristic approach that compared tag-sampled temperature data with available remotely-sensed sea surface temperature (SST) data in the area from 31–38°N and 118–125°N. This identified 'permissible locations' where the squid could have been each day before the pop-up day (e.g. the last day of deployment,  $D$ ) by excluding grid-cells that were too warm or too cold. Each permissible location did not have equal likelihood of squid occupancy because of the distances required to reach the pop-up location during the remaining time of the deployment. Relative weights for each permissible location were calculated based on distances required to reach past and future permissible locations as described below.

For each permissible location  $g$  on a given day  $t$  ( $g_t$ , where  $t = 1, 2, \dots, D$ ), a set of permissible locations for days before ( $B_t$ ) and after ( $A_t$ )  $t$  was identified, as described by the time lapse  $\delta$  relative to  $t$  (where  $\delta = \dots, -2, -1, 0, 1, 2, \dots$ ). Thus,  $S_{t+\delta}$  was the set of all permissible locations at time  $t + \delta$ , and  $g_t$  is any permissible location at time  $t$  ( $g_t$  belongs to the set  $S_t$ , which is denoted as  $g_t \in S_t$ ). The total number of permissible locations within  $S_{t+\delta}$  was designated as  $C_{t+\delta}$ .

$R_{t+\delta}(g)$  is the number of permissible locations at time  $t + \delta$  that are within a circle centered at  $g_t$  and whose radius is  $|\delta| \times V$ , where  $|\delta|$  is the absolute value of  $\delta$  and  $V$  is the maximum speed.

The suitability of permissible locations in the  $|\delta|$  vicinity of  $g_t$  is described before and after day  $t$  as:

$$B_t(g) = \frac{R_1(g)}{C_1} \times \frac{R_2(g)}{C_2} \times \dots \times \frac{R_{t-1}(g)}{C_{t-1}} \quad (1)$$

and

$$A_t(g) = \frac{R_{t+1}(g)}{C_{t+1}} \times \dots \times \frac{R_{D-1}(g)}{C_{D-1}} \times \frac{R_D(g)}{C_D} \quad (2)$$

Each component in  $A_t(g)$  is a single value in relation to day  $t$  that will have a value close to 1 if all permissible cells could be reached from  $g_t$ , a value close to 0 if few could be reached from  $g_t$ . Values for each day relative to  $t$  are multiplied together, and, thus, the overall value of  $A_t(g)$  will be higher if  $g_t$  is in a location where it will reach many locations in later days. This same logic applies to  $B_t(g)$ , which compares  $g_t$  to previous days.

Following the calculations of  $B_t(g)$  and  $A_t(g)$ , each permissible location on a given day was assigned a relative weight  $W[g_t]$  by computing the product of  $B_t(g)$  and  $A_t(g)$  and dividing by  $N_t$ , a normalizing constant that guarantees the weights of all locations at time  $t$  sum to one:

$$W[g_t] = \frac{B_t(g) \times A_t(g)}{N_t} \quad (3)$$

where

$$N_t = \sum_{g \in S_t} B_t(g) \times A_t(g) \quad (4)$$

Distances between each permissible location were then multiplied by the weighted value for each location to calculate weighted averages of daily velocities and distances from the 500 m contour line.

#### Tag-sampled temperature

Humboldt squid often swim to shallow depths above the thermocline at night as part of their daily vertical migration, although they can also occupy these depths during the day, particularly in the CCS where temperature in the surface mixed-layer is relatively cool (Stewart et al. 2012). If these depths were <25 m, we assumed that temperature at the squid's depth was approximately equal to SST. A map of depth at the thermocline was calculated and plotted as described elsewhere

(Staaf et al. 2011), and the 25 m definition appeared to be valid for all coastal areas off California during the period of study except for the region around Point Conception where it was slightly deeper (Fig. 2).

To compare tag-sampled temperature values to remotely-sensed SST data, the temperature range defined by the 5 shallowest depths recorded by the squid in each 24 h period was used to identify grid-cells where the squid could have been based on temperature alone. On a few days the squid did not reach depths shallower than 25 m, and in those cases the temperature values for the shallowest depths available were used. Thus, on these days temperature sampled by the squid would have been somewhat lower than the SST estimate, but were the only data available (see Appendix 1 for daily depth and temperature values).

#### Setting maximum sustained speed $V$

Maximum sustained speed,  $V$ , bounded the squid's maximum daily velocity that set the total daily distance traveled throughout the deployment period. Because maximum sustained swimming speed for Humboldt squid is unknown, we designated a value for  $V$  based on distances calculated between permissible locations. A minimum value for  $V$  of 55 km d<sup>-1</sup> was identified in this way, primarily from the set of permissible locations for tag CCS-5 during the last few days of the deployment period (see 'Results: Tagging'). Higher values of  $V$  were also investigated, but 55 km d<sup>-1</sup> was found to be the most conservative upper limit (Table 2).

Distances between permissible locations on each day were then weighted by calculating distances as described above to calculate average daily velocities and average distances off the shelf (calculated from the 500 m isobath). These results are reported and discussed as 'model' values.

#### Horizontal distance calculations and vertical habitat

Distances between permissible locations on each day were then weighted by calculating distances as described above to calculate average daily velocities and average distances off the shelf (calculated from

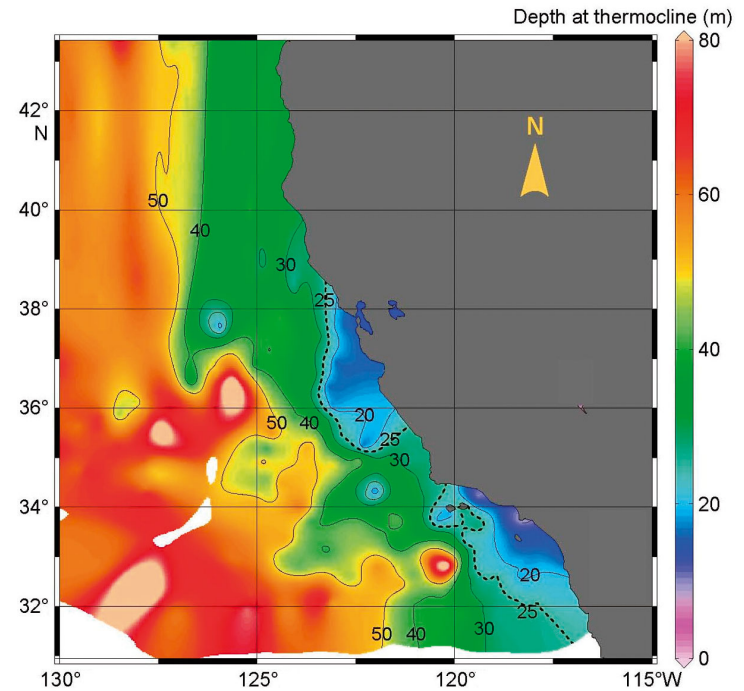


Fig. 2. Mixed layer depths (thermocline) mapped in the California Current System. Contour depths are shown with solid lines, with the 25 m contour marked with a dashed line. The mean depth of the thermocline in the relevant region off California during November (averaged from 2005–2009) was ~20–30 m, and we take this depth to approximate the mixed-layer depth. Thus, temperatures sampled by squid at depths shallower than 25 m were assumed to represent surface temperatures and to thus be comparable to remotely sensed SST. Data are from the World Ocean Database ([www.nodc.noaa.gov](http://www.nodc.noaa.gov)) averaged from 2005–2009 as described in the text

Table 2. Setting maximum speed,  $V$ . Maximum speed was set to  $V = 55$  km d<sup>-1</sup> in order for the model to run when few permissible locations occurred on a given day. Higher values of  $V$  were also investigated to see if this would reduce the maximum velocity calculated by the model, but this increased mean and max velocities. Thus, 55 km d<sup>-1</sup> was deemed to be the most conservative value for the present study

Maximum speed $V$ (km d <sup>-1</sup> )	Velocity (km d <sup>-1</sup> ) Mean	Velocity (km d <sup>-1</sup> ) Max	Total distance (km) Mean
55	$38.9 \pm 5.6$	51.9	660.6
80	$55.2 \pm 4.8$	66.5	938.6
100	$66.8 \pm 5.1$	81.6	1136.1

the 500 m isobath). Overall averages were also calculated for each day. These results are reported and discussed as 'model' values. A simple illustrated example of the model can be found in Stewart (2012).

Vertical depth and temperature data were also investigated for each tag on a daily basis to identify patterns in daytime percent time-at-depth and maxi-

mum depth. We were particularly interested to see any changes in diel vertical migratory behavior in association with horizontal migrations. Temperature data were also investigated at daytime and nighttime depths.

### Environmental data

NOAA's Xtractomatic data client was used to access remotely-sensed environmental data from the NOAA Coastwatch website (<http://coastwatch.pfel.noaa.gov/xtracto/>) for the tagging area (31–38°N and 118–125°N) in  $0.1^\circ \times 0.1^\circ$  grid-cells ( $= 11 \times 11$  km grid-cells) for each day of the study period. SST data were selected as a 5 d blended composite of MODIS, AMSRE, GOES and AVHRR, which provided the finest spatial and temporal resolution suitable for this study. Bathymetry data used to define the 500 m contour were accessed on the same resolution and area using the ETOPO1 data set (Amante & Eakins 2009, [www.ngdc.noaa.gov/mgg/bathymetry](http://www.ngdc.noaa.gov/mgg/bathymetry)).

Analyses were performed with MATLAB 7.9.0 (Mathworks), R 2.11 (<http://cran.r-project.org>) and Fortran 95 and Ocean Data View (Schlitzer 2012, [odv.awi.de](http://odv.awi.de)). All arc distances were computed with the Haversine formula, which calculates distances between points on a sphere, assuming the earth is a perfect sphere of radius 6378 km (Sinnott 1984) and are called horizontal distances. Maps were created using ArcGIS 10.0 (ESRI). All environmental data were accessed in spring 2011.

## RESULTS

### Tagging

Data were obtained from 5 of the 9 tags deployed in California (Fig. 1, Table 1) for a total of 41.7 d of sampling. Only one tag popped up at the programmed time; all other tags reported prematurely. Although this is a common occurrence with tagging squid (Gilly et al. 2006, Bazzino et al. 2010), the cause for premature release of any tag is unknown. Presumably a tag can be shed either through mechanical failure of the attachment to the flapping fin or in conjunction with attacks by other squid or large predators.

Pop-up locations were all south or southwest, with 3 over the shelf and 2 offshore (Fig. 1). All tagged squid made diel migrations at dusk from mean daytime depths of ~360 m to nighttime near-surface

depths throughout the deployment. There was considerable variability in both maximum daytime and minimum nighttime depths and range of the water column occupied by individual squid on any given day or night (Fig. 3A,C,E). Individual squid reached depths shallower than the 25 m thermocline during 75 to 100 % of their days at liberty.

The tag on CCS-5 popped up ~600 km from the deployment location, indicating that this squid swam at least this distance in its 17.6 d deployment, yielding a minimum daily (direct) velocity of  $34.0 \text{ km d}^{-1}$ , similar to minimum daily velocities previously reported (Gilly et al. 2006). Thus, the set maximum velocity parameter ( $55 \text{ km d}^{-1}$ ) eventually used to model daily locations was a 38 % increase from this minimum, empirically determined value.

### Daily movement

Model results demonstrated movement similar to the direct pathways between deployment and pop-up locations for 4 of the 5 tagged squid. CCS-3 and CCS-5 demonstrated this well: the estimated daily positions are consistent with the direct pathways, and the model further provides estimates on daily velocities and potential offshore movement. Model results for CCS-1 and CCS-4 also were consistent with direct distances, although their deployments were  $\leq 3$  d and data from these tags will not be considered in detail (see Table 3). In the case of CCS-2, in which a relatively long deployment yielded a small direct distance, the model provided valuable estimates that are not evident from the deployment and pop-up coordinates alone. CCS-3, CCS-5, and CCS-2 are discussed individually below.

CCS-3 carried the PAT tag for 5.7 d and swam offshore, with a direct distance between deployment and pop-up locations of 118.2 km. The model indicated a total distance of 182.2 km (Table 3; Fig. 4; see also Video S1 at [www.int-res.com/articles/suppl/m471p135\\_supp/](http://www.int-res.com/articles/suppl/m471p135_supp/)) at a velocity of  $36.4 \pm 1.6 \text{ km d}^{-1}$  (mean  $\pm$  SD) and a maximum velocity of  $38.8 \text{ km d}^{-1}$  on Day 2 (Fig. 5A). Movement predicted by the model was more or less directly offshore (Fig. 5B). Although daily horizontal velocities were rather constant (Fig. 5A), daily daytime depths increased as the squid moved offshore (Fig. 3A). Daily nighttime temperatures became warmer with offshore movement although daily nighttime depths did not change (Fig. 3A,B). These features are consistent with the observed and calculated offshore movement.

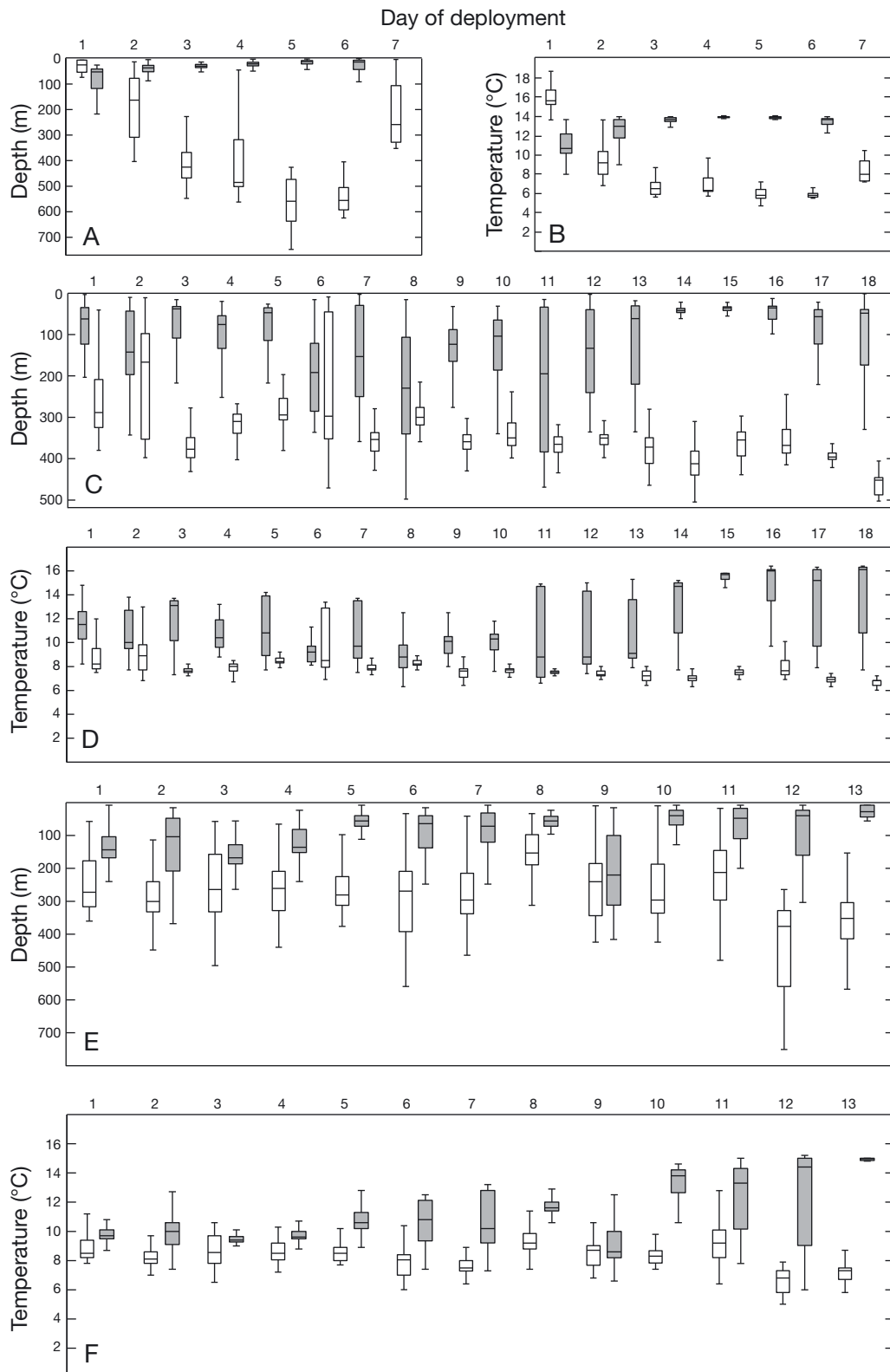


Fig. 3. *Dosidicus gigas*. Boxplots of daily depth and temperature data for 3 squid with the longest deployments: (A,B) CCS-3, (C,D) CCS-5 and (E,F) CCS-2. Open boxes show daytime information and shaded boxes show nighttime information: the boxes capture 50% of the data (the edges represent the 25th and 75th percentiles) with the median value indicated with a horizontal bar. The whiskers capture 99.7 % of the data. Outliers are not shown

Table 3. *Dosidicus gigas*. Distances and velocities. Direct measurements are based on deployment and pop-up information, and model measurements are estimates from the model. Mean model velocities are weighted means as described in 'Materials and methods: Movement analyses', and are the basis for total model distance. Distance from shelf is measured from the 500 m contour and positive values are on the shelf

Squid	Velocity ( $\text{km d}^{-1}$ )			Total dist. (km)		Dist. from shelf (km)	
	Direct Min	Model Mean	Model Max	Direct Min	Model Mean	Direct Min	Model Max
CCS-1	20.0	$42.4 \pm 3.4$	44.8	53.8	84.8	-55.1	-55.1
CCS-2	8.4	$34.7 \pm 2.3$	39.1	106.1	416.5	2.2	-30.7
CCS-3	20.7	$36.4 \pm 1.6$	38.8	118.2	182.2	-104.2	-104.2
CCS-4	14.9	$34.5 \pm 2.2$	36.5	44.7	103.5	-7.8	-16.5
CCS-5	34.0	$38.9 \pm 5.6$	51.9	599.2	660.6	-50.0	-66.9

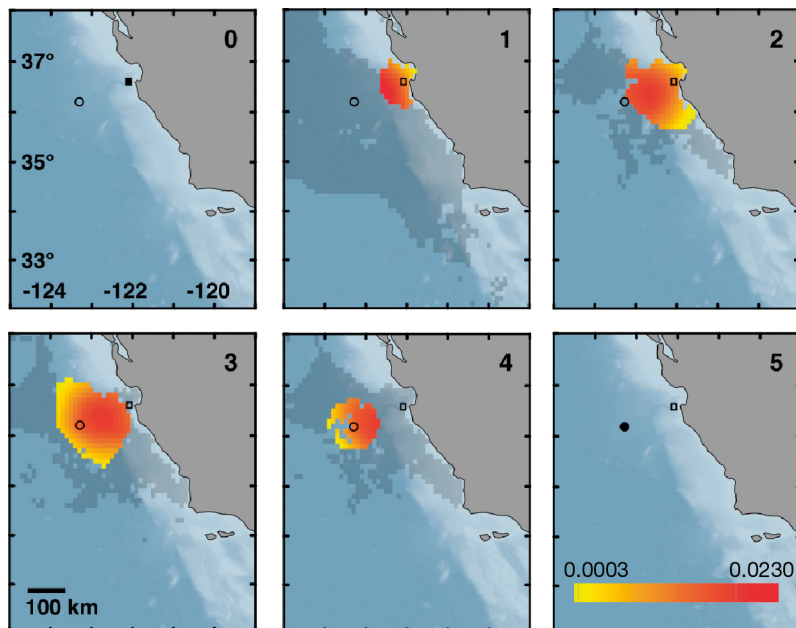


Fig. 4. *Dosidicus gigas*. Possible daily locations (0–5) for CCS-3 as estimated by the model. Colored pixels show the locations with highest (red) to lowest (yellow) weights based on model output. Permissible locations based solely on SST (but not probable based on distance traveled, see 'Materials and methods: Movement analyses') are shown transparently in gray. Integers indicate the deployment day. Deployment (square) and pop-up (circle) locations are shown in each panel, and are filled in on Days 0 and 5, respectively

CCS-5 had a direct distance of 599.2 km, corresponding to a minimum sustained swimming rate of  $34.0 \text{ km d}^{-1}$  (Table 3). The model suggested a southward migratory route that was consistent with the direct distance, with potential movement up to 50 km off the shelf (Fig. 6; Video S2). Modeled total distance for CCS-5 was 660.6 km at a mean velocity of  $38.9 \pm 5.6 \text{ SD km d}^{-1}$  and a maximum of  $51.9 \text{ km d}^{-1}$ . CCS-5's daily velocity was rather constant throughout the deployment but increased after Day 15

(Fig. 5C), just before the tag popped up. Daily daytime depths had a narrow range, with depths never exceeding 500 m, while nighttime depths had a much wider range (Fig. 3C). A narrow daytime temperature band ( $7$  to  $8^\circ\text{C}$ ) was associated with the entire deployment (excluding days where the depth range was also wider), and nighttime temperatures increased after Day 11 as CCS-5 entered the Southern California Bight (Fig. 3D).

The direct distance between deployment and pop-up location for CCS-2 was 106.1 km, giving a minimum average velocity of  $8.4 \text{ km d}^{-1}$  south during its 12.7 d deployment. This velocity was much lower than observed in any other squid, and the model predicted that squid CCS-2 initially swam north along the shelf and then turned to swim south, past the area of tag deployment (Fig. 7; Video S3). This trajectory corresponds to a total distance traveled of  $>415 \text{ km}$  at a velocity of  $34.7 \pm 2.3 \text{ km d}^{-1}$  (Fig. 5E). The model suggests that velocities during the movement north and south were similar, with greater potential for offshore movement (up to 30 km from the shelf) when the squid swam south (Fig. 5E,F). Daily daytime depths were always  $<500 \text{ m}$  except on Days 11 to 12 just before the tag popped up (Fig. 3E). The predicted movement south also corresponded with warmer nighttime temperatures (Fig. 3F).

## DISCUSSION

### Horizontal migration

This study provides the first information on horizontal movements of Humboldt squid in the CCS and yields new estimates of sustained daily velocities and migratory capabilities of this species. Based on information from 5 PAT tags deployed off central California, we report that Humboldt squid can swim at a speed of  $\sim 39 \text{ km d}^{-1}$  for at least 17 d, which is the longest sustained movement recorded. Humboldt squid traveling at such speeds maintain typical diving behavior by making diel vertical migrations from

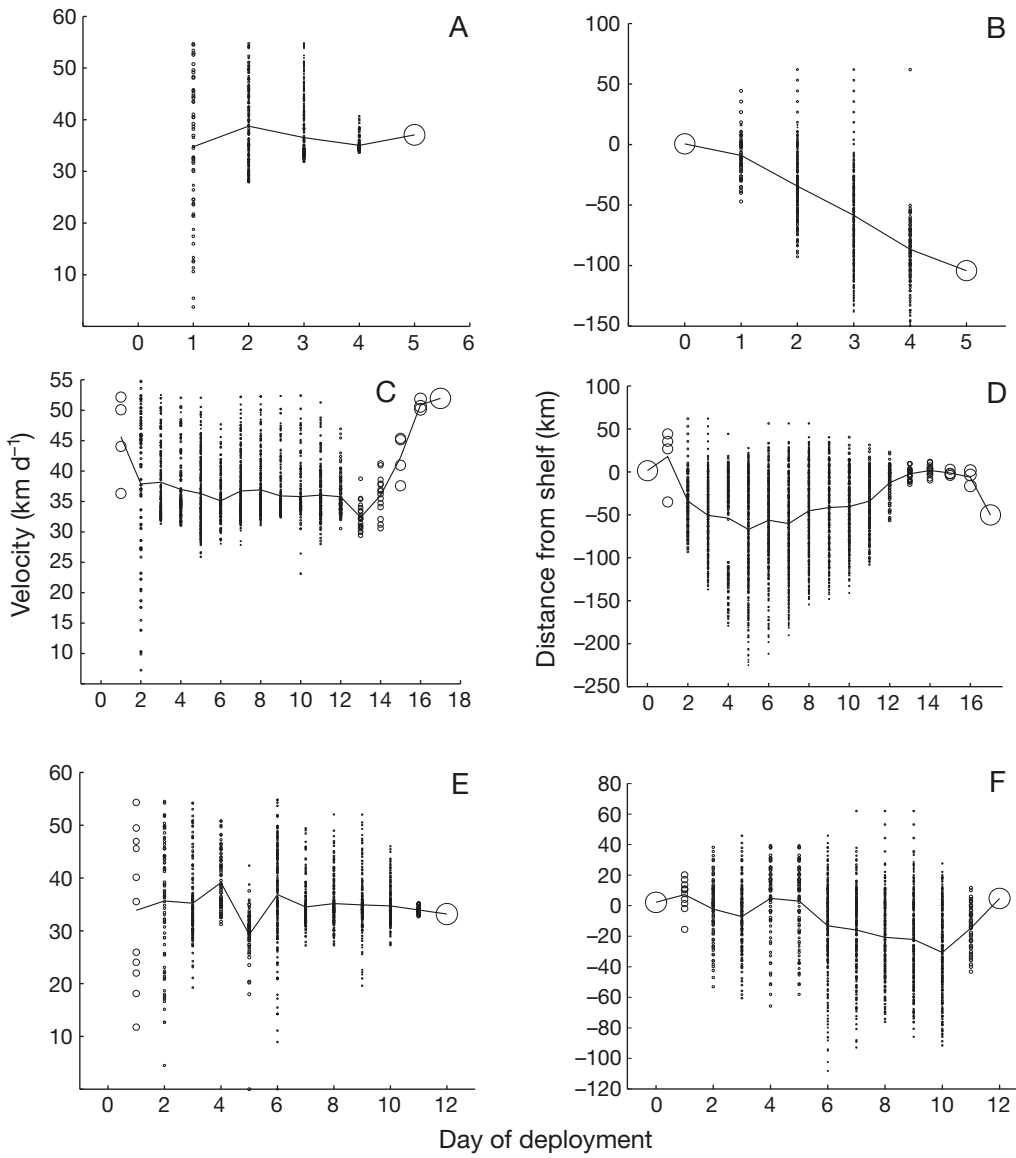


Fig. 5. *Dosidicus gigas*. Daily weighted values for distances traveled by 3 tags. Circle sizes show the weight (0–1), and black lines show the weighted mean for each day. (A) CCS-3 velocity; (B) CCS-3 distance from the shelf (500 m isobath); (C) CCS-5 velocity; (D) CCS-5 distance from the shelf; (E) CCS-2 velocity; (F) CCS-2 distance from the shelf. (B,D,F) Positive values indicate the squid was on the shelf and negative values indicate it was offshore

>300 m during the day to <50 m at night (Fig. 3; Stewart et al. 2012). In addition, despite short deployment times, all squid tagged in the autumn swam south or west, consistent with the hypothesis that squid return to Mexico, or potentially to offshore waters, to spawn in a suitable habitat (Staaf et al. 2011, Field et al. 2012).

We used a simple modeling approach to estimate daily mean positions of the squid throughout each tag deployment. Estimated mean daily velocities of all squid were also ~37 km d<sup>-1</sup>, similar to the direct rate cited above for CCS-5 and to previous reports of

~100 km distances in 3 d (Gilly et al. 2006). Daily velocities were calculated from estimated daily locations and were consistent with the direct pathways assumed from deployment and pop-up positions for all tags except CCS-2 (Table 3).

CCS-2 is the only case where the model predicted a trajectory that significantly differed from that inferred from the direct route between tag deployment and pop-up locations. The direct distance and deployment time for this squid yield a daily velocity of <10 km d<sup>-1</sup>, which is much lower than the minimum direct velocities for the other 4 squid. The

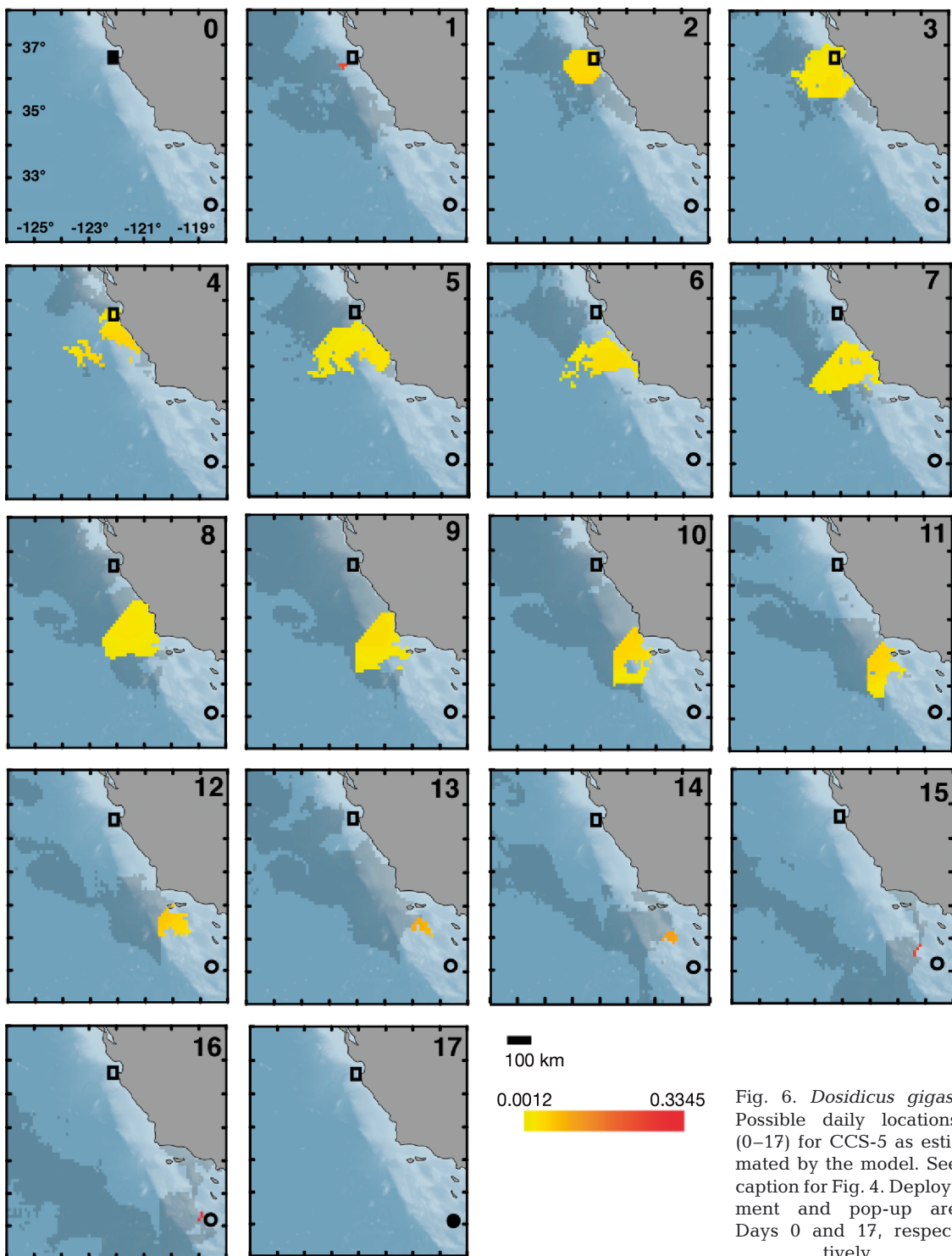


Fig. 6. *Dosidicus gigas*. Possible daily locations (0–17) for CCS-5 as estimated by the model. See caption for Fig. 4. Deployment and pop-up are Days 0 and 17, respectively

model suggests that this squid swam north for several days before returning south, past the deployment location. Therefore, the model provided insight on potential movement that was not otherwise evident. The model also suggests that CCS-2 stayed near the

shelf during most of its deployment. This is consistent with its daytime depth distributions that were shallower and similar to those of CCS-5, a squid that also probably stayed near the shelf during its deployment.

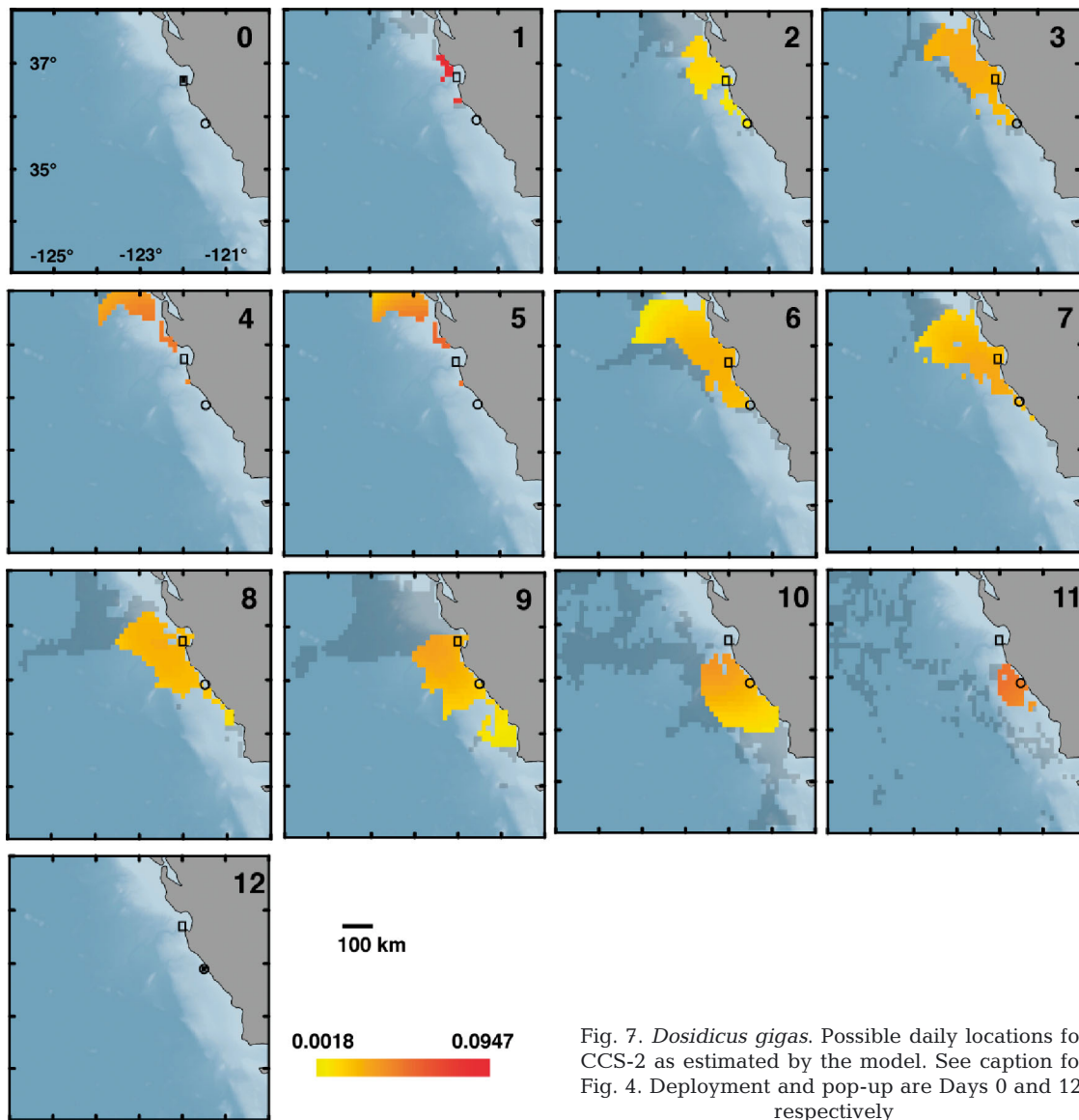


Fig. 7. *Dosidicus gigas*. Possible daily locations for CCS-2 as estimated by the model. See caption for Fig. 4. Deployment and pop-up are Days 0 and 12, respectively

### Tracking and modeling marine animal movements

In this study, we took a heuristic approach to uncover general patterns in movement (i.e. south, north, or offshore) as the first attempt to model Humboldt squid migration. State-space modeling, an approach widely used for animal geolocation studies, relies on observed position data with error distributions to estimate unobservable, true positions, or states, of animals (e.g. Jonsen et al. 2003). These observed positions and associated error distributions are usually either latitude and longitude estimates transmitted to Argos (Jonsen et al. 2003, 2005) or based on light data collected by the tags at the surface (where longitude

is estimated from the light intensity at local noon and latitude is estimated from estimates of local day length) (e.g. Sibert et al. 2003, Nielsen et al. 2006, Lam et al. 2008, Patterson et al. 2008).

Several studies have used a state-space approach without such geolocation data, and instead have created models using tidal data (Hunter et al. 2003, Pedersen et al. 2008), salinity data (Andersen et al. 2007) or estimates of sunrise and sunset based on animal diving behavior (Green et al. 2009). However, we chose a more heuristic approach largely due to the constraints inherent to our data that do not have geolocation estimates or associated error distributions based on light data (because of deep daytime depths

occupied by Humboldt squid) or Argos positions (other than deployment and pop-up locations). Furthermore, our short deployment periods (3 to 17 d) and small deployment scales (50 to 600 km) occur close to the coastline. Error estimates associated with state-space models can be over 50 km for migratory marine animals (e.g. Green et al. 2009) and such resolution would not provide informative results in our situation.

Results using our simple modeling approach were in most cases consistent with observed deployment and pop-up locations, but modeling also suggested daily positions between these 2 points. There are 3 main consistencies in the model's output that give us confidence in its estimates. First, in all cases the model predicted daily mean velocities of  $\sim 37 \text{ km d}^{-1}$ , a value similar to that directly measured with the tags (Table 3) and to previous studies (Gilly et al. 2006). Second, in 4 of 5 cases, the model provided daily position estimates that were consistent with the direct pathway between the tags' deployment and pop-up locations. Third, model estimates of daily positions are generally consistent with daily daytime depth distributions. Squid seem to occupy deeper depths during the daytime when the bathymetry allows, and generally show deeper daytime depths as they move into deeper waters (Gilly et al. 2006, Bazzino et al. 2010). Thus, the progressively deeper daytime depths seen with CCS-3 (Fig. 3A) are consistent with offshore movement (Fig. 4), and the shallower daytime depths of CCS-2 and CCS-5 (Fig. 5C) are consistent with remaining near the shelf during the deployments. Although in the case of CCS-5, the modeled trajectory could be reasonably inferred from the deployment and pop-up locations, this was clearly not the case for CCS-2. Instead, the output from the model revealed a rather extensive north-south movement at a velocity comparable to that shown by the other squid.

This study does lay the groundwork for future modeling of Humboldt squid in a state-space framework. As tag deployment methods evolve, squid could potentially be tracked during much longer deployment periods and distances. Additionally, ground-truthing the model using available hydrographic data collected *in situ* could increase confidence in model output. This was attempted in this study by comparing the vertical diving profiles of CCS-5 in the Southern California Bight with CalCOFI (California Cooperative Oceanic Fisheries Investigations, [www.calcofi.org](http://www.calcofi.org)) surveys that were carried out in the same area at that time (not illustrated). Incorporating these data into a modeling approach, potentially along

with velocities of currents, both near-surface and at depth, would improve our understanding of squid movement.

### Diving behavior and total velocities

Daily horizontal velocities estimated in this study are likely to underestimate the true capability of Humboldt squid, because vertical movements have been ignored in the model. All squid in this study made diel vertical migrations to and from near-surface waters to depths of  $\sim 350$  to 600 m, which adds  $\sim 1$  km to the total daily distance covered, and some reached depths  $>1200$  m (Stewart et al. 2012). In addition, squid often showed rapid vertical transitions during both day and night. For example, daytime movements on Days 2 and 6 of CCS-5's deployment involved many vertical excursions of  $>250$  m (Fig. 3C), but this diving behavior was not reflected in the mean velocity for those days (Fig. 5C).

Although vertical movements might be expected to lead to a decrease in total horizontal movement possible in a day, the effect is difficult to quantify. Climb-and-glide swimming (active vertical jetting and essentially passive sinking with velocities from  $-0.15$  to  $+0.05 \text{ m s}^{-1}$ ) accounts for 80 % of a tagged squid's time, and the total horizontal component of this behavior has been estimated to be up to  $20 \text{ km d}^{-1}$  (Gilly et al. 2012). How much of this motion is unidirectional is unknown, but the potential for a significant net contribution to horizontal movement with minimal energy expenditure is an inherent feature of the squid's style of locomotion.

Horizontal velocities might be further underestimated because they do not incorporate any amount of time spent foraging, an activity that can occur at depth during the day (Zeidberg & Robison 2007) and near the surface at night (Benoit-Bird & Gilly 2012) depending on food availability. In the CCS, Humboldt squid forage on both mesopelagic microneuston as well as coastal organisms that inhabit shallower depths (Field et al. 2007, 2012), and the latter organisms are presumably encountered by squid at shallower depths at night. Humboldt squid caught at the location and time of tagging in November 2009 had stomachs full of both mesopelagic and coastal organisms (Field et al. 2012), and, thus, it is likely that tagged squid were also foraging during the migration south. It is not known whether the majority of horizontal migration occurs during the day or at night, or how this activity might be curtailed by or combined with foraging.

### Swimming with and against currents

Diel vertical migrations expose Humboldt squid to opposing currents at different depths, the intensity and flow geography of which change seasonally (Agostini et al. 2006). The California Current, which flows equatorward from the surface to ~500 m deep, is strongest in the summer and early autumn (Bograd et al. 2010) and has an average speed of 0.1 m s<sup>-1</sup>, or 8.6 km d<sup>-1</sup> (Denny 2008). Thus, if a Humboldt squid migrates south at an average speed of 37 km d<sup>-1</sup>, the California Current could account for ~25 % of the distance traveled. Thus, while the California Current may facilitate energy conservation, Humboldt squid appear to swim at rates that considerably exceed the velocity of water flow.

In addition, the diel vertical migrations of Humboldt squid may take it out of the shallower equatorward-flowing California Current and into the deeper poleward-flowing California Undercurrent/Davidson Current. Perhaps during southward migrations in late autumn Humboldt squid save energy actively swimming with the California Current at nighttime and then against the weaker California Undercurrent during the day.

### Humboldt squid in the CCS

This study takes an important first step towards elucidating the movement patterns and swimming velocities of Humboldt squid in the CCS, where they are known to interact with many predator and prey species. Our results demonstrate that *Dosidicus gigas* is capable of sustaining average horizontal swimming speeds of ~37 km d<sup>-1</sup> and suggest a maximum horizontal speed of >50 km d<sup>-1</sup>, but it is likely that these values are underestimations of the actual swimming capabilities when current speeds, vertical velocities, and foraging are taken into account. Interpreting diving behavior and how it relates to horizontal migration is difficult and defines an important challenge for further studies of Humboldt squid movement.

At the horizontal velocities suggested in this study, swimming the 2750 km between Baja California and British Columbia could be accomplished by Humboldt squid in ~65 to 80 d each direction, ~75 % of which would be spent in US waters in addition to any time spent in other areas along the way. Humboldt squid are observed in large numbers off central California for ~6 mo each year (Zeidberg & Robison 2007, Stewart 2012), presumably as they move north to

British Columbia and then back south (Field et al. 2012). An alternative migration during the same seasonality has also been hypothesized to involve a proposed spawning habitat that appears well offshore of the California coast between July and October (Staaf et al. 2011). Velocities and trajectories of horizontal movements identified in this study would be consistent with either of these migrations. Further tagging studies and new modeling applications will be valuable in defining these putative spawning migrations, both of which may be expected to shift to more northern latitudes as long-term warming of oceanic waters (Doney et al. 2012, Salvadeo et al. 2011) and northward expansion of the subtropical Pacific biome (Polovina et al. 2011) continue.

**Acknowledgments.** We thank our colleagues who helped with tagging and recovery operations: J. Field, K. Baltz, A. Booth, I. Wilson, and M. Paull. We also thank A. Booth, R. deLemos and R. Mendelsohn for programming help and D. Staaf, L. Zeidberg, P. Daniel, H. Bailey, S. Jorgensen and 3 anonymous reviewers for technical support and comments on the manuscript. The Monterey Bay National Marine Sanctuary allowed use of several research vessels and the captains and crews provided outstanding operational support. Pathfinder SST was provided courtesy of NOAA's National Oceanographic Data Center and the University of Miami. Geostationary SST data were provided courtesy of NOAA NESDIS | OSDPD. MODIS SST data were provided courtesy of NASA | GSFC | Ocean Biology Products Group. AMSR-E SST data were provided courtesy of Remote Sensing Systems, Inc. (Santa Rosa, CA). This work was conducted under the California Department of Fish and Game permit SC-009763 to J.S.S. and supported by grants from California Sea Grant and California Ocean Protection Council (R/OPCFISH-06) and the National Science Foundation (OCE 0850839).

### LITERATURE CITED

- Agostini V, Francis RC, Hollowed AB, Pierce SD, Wilson C, Hendrix AN (2006) The relationship between Pacific hake (*Merluccius productus*) distribution and poleward subsurface flow in the California Current System. Can J Fish Aquat Sci 63:2648–2659
- Amante C, Eakins BW (2009) ETOPO1 1 Arc-minute global relief model: procedures, data sources and analysis. NOAA Tech Memo NESDIS NGDC-24
- Andersen KH, Nielsen A, Thygesen UH, Hinrichsen HH, Neuenfeldt S (2007) Using the particle filter to geolocate Atlantic cod (*Gadus morhua*) in the Baltic Sea, with special emphasis on determining uncertainty. Can J Fish Aquat Sci 64:618–627
- Bazzino G, Gilly WF, Markaida U, Salinas-Zavala CA, Ramos-Castillejos J (2010) Horizontal movements, vertical-habitat utilization and diet of the jumbo squid (*Dosidicus gigas*) in the Pacific Ocean off Baja California Sur, Mexico. Prog Oceanogr 86:59–71
- Benoit-Bird K, Gilly WF (2012) Coordinated nocturnal behavior of foraging jumbo squid *Dosidicus gigas*. Mar Ecol Prog Ser 455:211–228

- Block BA, Jonsen ID, Jorgensen SJ, Winship AJ and others (2011) Tracking apex marine predator movements in a dynamic ocean. *Nature* 475:86–90
- Bograd SJ, Castro CG, Di Lorenzo E, Palacios DM, Bailey H, Gilly WF, Chavez FP (2008) Oxygen declines and the shoaling of the hypoxic boundary in the California Current. *Geophys Res Lett* 35 L12607, doi:10.1029/2008GL034185
- Bograd SJ, Schroeder I, Sarkar N, Qiu X, Sydeman WJ, Schwing FB (2009) Phenology of coastal upwelling in the California Current. *Geophys Res Lett* 36:L01602, doi: 10.1029/2008GL035933
- Bograd SJ, Sydeman W, Barlow J, Booth A, Brodeur R, and 29 others (2010) Marine ecosystems of the North Pacific Ocean 2003–2008. PICES Special Publication 4:106–141
- Boucharel J, Dewitte B, Penhoat Y, Garel B, Yeh SW, Kug JS (2011) ENSO nonlinearity in a warming climate. *Clim Dyn* 37:2045–2065
- Braid HE, Deeds J, DeGrasse SL, Wilson JJ, Osborne J, Hanmer RH (2012) Preying on commercial fisheries and accumulating paralytic shellfish toxins: a dietary analysis of invasive *Dosidicus gigas* (Cephalopoda: Ommastrephidae) stranded in Pacific Canada. *Mar Biol* 159:25–31
- Brodeur R, Ralston S, Emmett R, Trudel M, Auth T, Phillips A (2006) Anomalous pelagic nekton abundance, distribution, and apparent recruitment in the northern California Current in 2004 and 2005. *Geophys Res Lett* 33: L22S08, doi:10.1029/2006GL026614
- Camarillo-Coop S, De Silva-Dávila R, Hernández-Rivas ME, Durazo-Arvizu R (2007) Distribution of *Dosidicus gigas* paralarvae off the west coast of the Baja California peninsula, Mexico. In: Olson RJ, Young JW (eds) The role of squid in open ocean ecosystems. GLOBEC Report 24, Honolulu, HI, p 7–8.
- Chavez FP, Ryan J, Lluch-Cota S, Niñuen MC (2003) From anchovies to sardines and back: multidecadal change in the Pacific Ocean. *Science* 299:217–221
- Choi J, Soon-II A, Kug JS, Yeh SW (2011) The role of mean state on changes in El Niño's flavor. *Clim Dyn* 37: 1205–1215
- Cosgrove JA (2005) The first specimens of Humboldt squid in British Columbia. PICES Press 13:30–31
- Denny MW (2008) How the ocean works: an introduction to oceanography. Princeton University Press, Princeton, NJ
- Deutsch C, Brix H, Ito T, Frenzel H, Thompson L (2011) Climate-forced variability of ocean hypoxia. *Science* 333: 336–339
- Doney SC, Ruckelshaus M, Duffy JE, Barry JP and others (2012) Climate change impacts on marine ecosystems. *Ann Rev Mar Sci* 4:11–37
- Edwards M, Richardson A (2004) Impact of climate change on marine pelagic phenology and trophic mismatch. *Nature* 430:881–884
- Emmett RL, Brodeur RD, Miller TW, Pool SS, Krutzikowsky GK, Bentley PJ, McCrae J (2005) Pacific sardine (*Sardinops sagax*) abundance, distribution, and ecological relationships in the Pacific Northwest. CCOFI Rep 46: 122–143
- FAO (Food and Agriculture Organization of the United Nations) (2012) FAO yearbook: fishery and aquaculture statistics 2010. [www.fao.org/fishery/publications/yearbooks/en](http://www.fao.org/fishery/publications/yearbooks/en)
- Field JC, Baltz KA, Phillips AJ, Walker WA (2007) Range expansion and trophic interactions of the jumbo squid, *Dosidicus gigas*, in the California Current. CCOFI Rep 48:131–146
- Field JC, Elliger C, Baltz KA, Gillespie GE and others (in press) (2012) Foraging ecology and movement patterns of jumbo squid (*Dosidicus gigas*) in the California Current System. *Deep-Sea Res II* doi: 10.1016/j.dsr2.2012.09.006
- FishStat (2012) Food and Agricultural Organization of the United Nations (FAO). Capture Production dataset for Area 67 accessed August 2012. [www.fao.org/fishery/statistics/software/fishstat/en](http://www.fao.org/fishery/statistics/software/fishstat/en)
- García-Reyes M, Largier J (2010) Observations of increased wind-driven coastal upwelling off central California. *J Geophys Res* 115:C04011, doi:10.1029/2009JC005576
- Gilly WF (2006) Spreading and stranding of Humboldt squid. In Ecosystem Observations for the Monterey Bay National Marine Sanctuary 2005: 25–26. Monterey Bay National Marine Sanctuary, Monterey, CA. <http://montereybay.noaa.gov/reports/2005/eco/harvestedsp.html>
- Gilly WF, Markaida U (2007) Perspectives on *Dosidicus gigas* in a changing world. In: Olson J, Young J (eds) The role of squid in open ocean ecosystems. GLOBEC Report 24, Honolulu, HI, p 81–90
- Gilly WF, Markaida U, Baxter C, Block B and others (2006) Vertical and horizontal migrations by the jumbo squid *Dosidicus gigas* revealed by electronic tagging. *Mar Ecol Prog Ser* 324:1–17
- Gilly WF, Zeidberg LD, Booth JAT, Stewart JS, Marshall G, Abernathy K, Bell LE (2012) Locomotion and behavior of Humboldt squid, *Dosidicus gigas* (d'Orbigny, 1835), in relation to natural hypoxia in the Gulf of California, Mexico. *J Exp Biol* 215:3175–3190
- Green J, Wilson R, Boyd I, Woakes A, Green C, Butler P (2009) Tracking macaroni penguins during long foraging trips using behavioural geolocation. *Polar Biol* 32: 645–653
- Holmes J, Cooke K, Cronkite G (2008) Interactions between jumbo squid (*Dosidicus gigas*) and Pacific hake (*Merluccius productus*) in the northern California Current in 2007. CCOFI Rep 49:129–141
- Hunter E, Aldridge J, Metcalfe J (2003) Geolocation of free-ranging fish on the European continental shelf as determined from environmental variables. *Mar Biol* 142: 601–609
- Iles AC, Gouhier TC, Menge BA, Stewart JS, Haupt AJ, Lynch MA (2012) Climate-driven trends and ecological implications of event-scale upwelling in the California Current System. *Glob Change Biol* 18:783–796
- Jackson GD, O'Dor RK (2007) Squid—the new ecosystem indicators. In: Olson J, Young J (eds) The role of squid in open ocean ecosystems. GLOBEC Report 24, Honolulu, HI, p 78–80
- Jonsen I, Myers R, Flemming J (2003) Meta-analysis of animal movement using state-space models. *Ecology* 84: 3055–3063
- Jonsen I, Flemming J, Myers R (2005) Robust state-space modeling of animal movement data. *Ecology* 86: 2874–2880
- Koslows J, Goericke R, Lara-Lopez A, Watson W (2011) Impact of declining intermediate-water oxygen on deep-water fishes in the California Current. *Mar Ecol Prog Ser* 436:207–218
- Lam CH, Nielsen A, Sibert JR (2008) Improving light and temperature based geolocation by unscented Kalman filtering. *Fish Res* 91:15–25
- Litz MNC, Phillips AJ, Brodeur RD, Emmett RL (2011) Sea-

- sonal occurrences of Humboldt squid (*Dosidicus gigas*) in the northern California Current System. CCOFI Rep 52:97–108
- Markaida U, Gilly W, Salinas-Zavala C, Rosas-Luis R, Booth J (2008) Food and feeding of jumbo squid *Dosidicus gigas* in the central Gulf of California during 2005–2007. CCOFI Rep 49:90–103
- Mazzillo FFM, Staaf DJ, Field JC, Carter ML, Ohman MD (2011) A note on the detection of the neurotoxin domoic acid in beach-stranded *Dosidicus gigas* in the Southern California Bight. CCOFI Rep 52:109–115
- Nielsen A, Bigelow KA, Musyl MK, Sibert JR (2006) Improving light-based geolocation by including sea surface temperature. Fish Oceanogr 15:314–325
- Nigmatullin CM, Nesis K, Arkhipkin A (2001) A review of the biology of the jumbo squid *Dosidicus gigas* (Cephalopoda: Ommastrephidae). Fish Res 54:9–19
- Parmesan C (2006) Ecological and evolutionary responses to recent climate change. Annu Rev Ecol Evol Syst 37: 637–669
- Patterson T, Thomas L, Wilcox C, Ovaskainen O, Matthiopoulos J (2008) State-space models of individual animal movement. Trends Ecol Evol 23:87–94
- Pedersen MW, Righton D, Thygesen UH, Andersen KH, Madsen H (2008) Geolocation of North Sea cod (*Gadus morhua*) using hidden Markov models and behavioural switching. Can J Fish Aquat Sci 65:2367–2377
- Perry AL, Low PJ, Ellis JR, Reynolds JD (2005) Climate change and distribution shifts in marine fishes. Science 308:1912–1915
- Polovina JJ, Dunne JP, Woodworth PA, Howell EA (2011) Projected expansion of the subtropical biome and contraction of the temperate and equatorial upwelling biomes in the North Pacific under global warming. ICES J Mar Sci 68:986–995
- Prete A, Soykan CU, Dewar H, Wells RJD, Spear N, Kohin S (2012) Comparative feeding ecology of shortfin mako, blue and thresher sharks in the California Current. Environ Biol Fishes 95:127–146
- Ramos-Castillejos JE, Salinas-Zavala CA, Camarillo-Coop S, Enríquez-Paredes LM (2010) Paralarvae of the jumbo squid, *Dosidicus gigas*. Invertebr Biol 129:172–183
- Salvadeo C, Lluch-Belda D, Lluch-Cota S, Mercuri M (2011) Review of long term macro-fauna movement by multi-decadal warming trends in the northeastern Pacific. In: Blanco J, Kheradmand H (eds) Climate change – geo-physical foundations and ecological effects. InTech, Rijeka, p 217–230
- Schlitzer R (2012) Ocean Data View User's Guide. [http://odv.awi.de/fileadmin/user\\_upload/odv/misc/odv4Guide.pdf](http://odv.awi.de/fileadmin/user_upload/odv/misc/odv4Guide.pdf)
- Sibert J, Musyl M, Brill R (2003) Horizontal movements of bigeye tuna (*Thunnus obesus*) near Hawaii determined by Kalman filter analysis of archival tagging data. Fish Oceanogr 12:141–151
- Sinnott RW (1984) Virtues of the Haversine. Sky Telescope 68:159
- Staaf D, Zeidberg L, Gilly W (2011) Effects of temperature on embryonic development of the Humboldt squid *Dosidicus gigas*. Mar Ecol Prog Ser 441:165–175
- Stewart JS (2012) Humboldt squid in the northern California Current System. PhD dissertation, Stanford University, California.
- Stewart IJ, Hamel OS (2010) Stock assessment of Pacific hake, *Merluccius productus*, (a.k.a. whiting) in U.S. and Canadian waters in 2010. Northwest Fisheries Science Center, NOAA, Seattle, WA. [www.pcouncil.org/wp-content/uploads/Pacific\\_Whiting\\_2010\\_Assessment.pdf](http://www.pcouncil.org/wp-content/uploads/Pacific_Whiting_2010_Assessment.pdf)
- Stewart JS, Field JC, Markaida U, Gilly WF (2012) Behavioral ecology of jumbo squid (*Dosidicus gigas*) in relation to oxygen minimum zones. Deep-Sea Res II. doi:10.1016/j.dsr2.2012.06.005
- Stramma L, Prince ED, Schmidtko S, Luo J and others (2012) Expansion of oxygen minimum zones may reduce available habitat for tropical pelagic fishes. Nature Climate Change 2:33–37
- Wing BL (2006) Unusual invertebrates and fish observed in the Gulf of Alaska, 2004–2005. PICES Press 14:26–28
- Yeh SW, Kug JS, Dewitte B, Kwon MH, Kirtman BP, Jin FF (2009) El Niño in a changing climate. Nature 461: 511–514
- Zeidberg LD, Robison B (2007) Invasive range expansion by the Humboldt squid, *Dosidicus gigas*, in the eastern North Pacific. Proc Natl Acad Sci USA 104:12948–12950

**Appendix 1.** Daily temperature information for the 5 shallowest depths each squid encountered. Var: variance

	Depth			Temperature		
	Min	Max	Var	Min	Max	Var
<b>CCS-1</b>						
1	4.5	4.7	0.0	14.4	14.4	0.00
2	21.6	22.3	0.2	11.5	11.5	0.00
3	6.5	6.8	0.0	12.2	12.2	0.00
4	14.6	16.8	2.6	12.5	12.5	0.00
<b>CCS-2</b>						
1	0.0	20.0	200.0	12.5	12.7	0.02
2	8.0	56.0	1152.0	10.8	13.1	2.65
3	16.0	24.0	32.0	12.7	13.1	0.08
4	16.0	40.0	288.0	10.9	11.9	0.50
5	24.0	40.0	128.0	11.0	11.7	0.25
6	8.0	16.0	32.0	11.9	12.8	0.41
7	16.0	24.0	32.0	12.2	12.5	0.05
8	8.0	8.0	0.0	12.9	13.2	0.05
9	8.0	24.0	128.0	12.4	13.8	0.98
10	8.0	24.0	128.0	13.7	14.8	0.61
11	8.0	8.0	0.0	14.5	14.6	0.01
12	8.0	8.0	0.0	14.1	15.0	0.41
13	8.0	8.0	0.0	15.0	15.2	0.02
<b>CCS-3</b>						
1	5.0	5.0	0.0	13.7	15.3	1.28
2	11.5	11.5	0.0	13.6	13.6	0.00
3	4.5	13.5	40.5	13.8	14.0	0.02
4	13.5	16.0	3.1	13.6	13.7	0.01
5	2.5	2.5	0.0	14.0	14.1	0.01
6	2.0	2.5	0.1	13.8	14.0	0.02
<b>CCS-4</b>						
1	1.0	13.5	78.1	13.6	17.0	5.78
2	2.5	13.0	55.1	13.9	14.1	0.02
3	1.0	1.5	0.1	13.3	13.4	0.01
4	1.0	1.5	0.1	13.3	13.3	0.00
<b>CCS-5</b>						
1	3.0	3.0	0.0	14.2	14.8	0.18
2	5.0	6.0	0.5	13.6	13.7	0.01
3	18.0	25.5	28.1	13.6	13.7	0.01
4	19.5	27.5	32.0	12.8	13.2	0.08
5	5.0	10.0	12.5	13.3	13.7	0.08
6	3.0	4.0	0.5	13.2	13.4	0.02
7	2.5	4.5	2.0	13.5	13.7	0.02
8	15.5	30.5	112.5	12.8	14.3	1.13
9	32.0	43.5	66.1	12.0	14.3	2.65
10	31.5	40.5	40.5	13.1	14.7	1.28
11	15.0	20.5	15.1	14.6	14.9	0.05
12	2.5	9.5	24.5	14.8	15.0	0.02
13	33.0	37.5	10.1	13.9	14.9	0.50
14	21.5	25.0	6.1	14.9	15.2	0.05
15	22.0	24.5	3.1	15.7	15.8	0.01
16	13.0	22.5	45.1	15.7	16.4	0.25
17	21.5	23.5	2.0	15.7	15.9	0.02
18	1.0	7.0	18.0	16.3	16.3	0.00